https://doi.org/10.1016/j.energy.2018.09.063

Investigating dehumidification performance of solar-assisted liquid desiccant dehumidifiers considering different surface properties

Chuanshuai Dong, Lin Lu *, Tao Wen

Department of Building Services Engineering, The Hong Kong Polytechnic University, Kowloon, Hong Kong SAR, China

Corresponding email: vivien.lu@polyu.edu.hk

Abstract

Solar-assisted liquid desiccant dehumidification is promising regarding its lower energy consumption. Surface properties of dehumidifiers critically influence the dehumidification performance. Therefore, this paper aims at investigating the influence of surface properties on dehumidification performance of falling film dehumidifiers. Three commonly-used plate dehumidifiers, i.e., Stainless steel plate dehumidifier, Titanium plate dehumidifier and Polytetrafluoroethylene plate dehumidifier, with distinctive surface properties were chosen for study. Surface free energy was measured to characterize the adhesion between liquid desiccant and solid surface. Then, the effect of surface properties on dehumidification performance was experimentally investigated. The experimental results indicated that surface wettability demonstrated positive effect on dehumidification performance by increasing wetting area and reducing falling film thickness. As surface free energy increased from 30.34 mJ/m^2 to 50.61 mJ/m^2, the moisture removal rate increased from 0.155 to 0.213 with the enhancing ratio of 37.4%. A novel mass transfer correlation was developed, among which surface free energy was introduced to consider the effect of surface properties on dehumidification performance. It is estimated that 9.6 % of the energy consumption could be saved by improving surface wettability of falling film dehumidifiers. This research is also very useful to other falling film applications, such as evaporators, condensers and chemical columns.

Keywords: Lower energy consumption; Liquid desiccant dehumidification; Surface free energy; Dehumidification performance; Solar-assisted liquid desiccant

Nomenclature

A	Wetting area	m^2	***Subscripts***	
C_p	Specific heat capacity	$kJ/(kg \cdot K)$	a	Air
h	Enthalpy	kJ/kg	Cal	Calculated
h_D	Mass transfer coefficient	$g/(m^2 \cdot s)$	Equ	Equilibrium status
m	Mass flow rate	kg/s	Exp	Experimental
m_ω	Moisture removal rate	g/s	f	Cooling water
T	Temperature	℃	in	Inlet
γ_L	Surface free energy of liquid	mJ/m^2	out	Outlet
γ_S	Surface free energy of solid	mJ/m^2	s	Solution
θ	Contact angle	°, rad	***Superscripts***	
η_ω	Dehumidification efficiency		D	Dispersive component
ω	Humidity ratio	g/kg	P	Polar component
$\triangle\omega$	Humidity difference	g/kg		

1. Introduction

As humidity can affect building structure as well as indoor air quality, it is very necessary to control the humidity of indoor air [1]. There exist several approaches to control air humidity, such as vapor condensation and solid adsorption [2], but these dehumidification methods consume large amount of energy in air dehumidification process. In Hong Kong, the commercial building sector takes up 43% of the whole energy consumption, among which air-conditioning system occupies around 25% [3], as shown in Fig. 1. In conventional vapor condensation dehumidification technology, the humid air is firstly cooled to dew point and the vapor is removed by condensation. Then, the dry air is reheated before being supplied to air-conditioned room. This process results in a lot of energy waste [4]. Besides, some severe environmental crisis such as the depletion of ozone layer might be caused by the Chlorofluoro Carbon (CFC) used in the vapor condensation air-conditioning system [5]. Therefore, new air dehumidification technology, i.e. solar-assisted liquid desiccant dehumidification, is regarded as a promising alternative due to less energy consumption and lower pollution [6, 7].

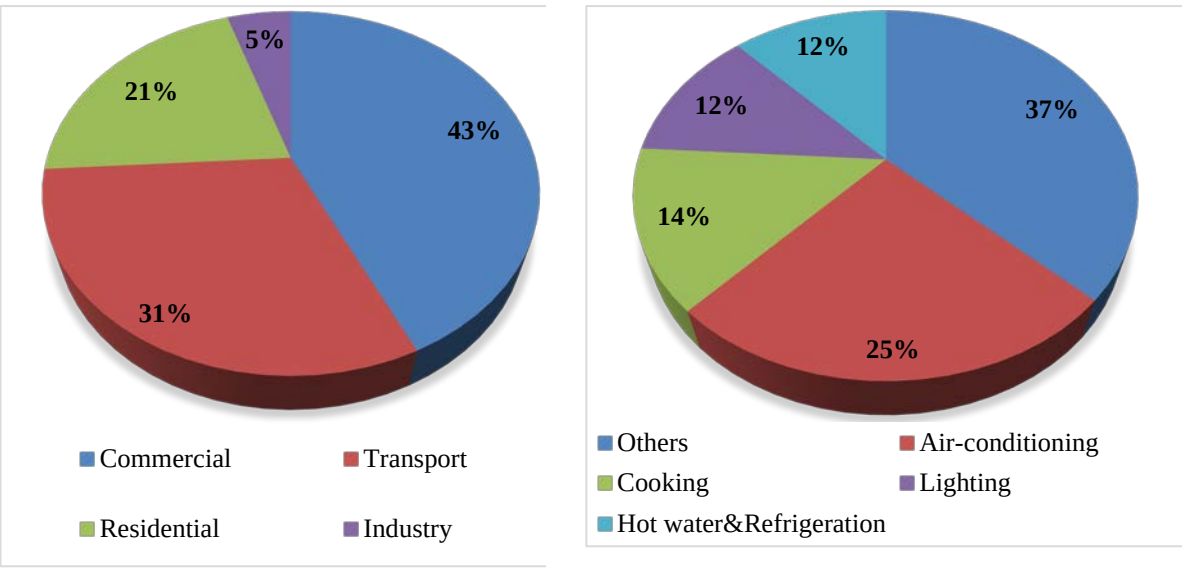

(a) Breakdown of total energy consumption

(b) Breakdown of energy consumption in commercial sector

Fig. 1 Hong Kong energy consumption analysis (2016)

In liquid desiccant air dehumidification system, humid air interacts with desiccant solution and the water vapor is absorbed by liquid desiccant due to pressure difference between humid air and saturated air above liquid desiccant [8]. As the main index for solar-assisted liquid desiccant dehumidifiers, dehumidification performance is influenced by several factors such as configurations of dehumidifiers, liquid desiccant types and operating conditions. Several liquid desiccants including glycols and halide salts such as triethylene glycol and LiCl, LiBr and $CaCl_2$ are commonly used [9]. The packing liquid desiccant dehumidifier, which is usually filled with different packings, is widely used for large surface area. Many researchers have investigated the dehumidification performance of packing dehumidifiers [10-12]. However, there exist several drawbacks in packing liquid desiccant dehumidifiers, such as liquid droplet carryover and high pressure drop, etc. Besides, the phase-change heat in dehumidification process might heat the liquid desiccant and deteriorate the absorption capacity.

To solve these problems, the internally-cooled falling film dehumidifier is drawing much attention. In falling film dehumidifier, the solution spreads out as thin film on plate surface. Then, the humid air interacts with thin falling film and the moisture exchanges from humid air to desiccant solution. Besides, the cooling fluid could remove the phase-change heat [13, 14]. The dehumidification characteristics of internally-cooled falling film dehumidifier have been investigated by many researchers. Cho et al. [15] investigated the combined heat/mass transfer performance in dehumidification process using a plate-type heat exchanger. Yin et al. [16] studied the dehumidifiers/regenerators of liquid desiccant cooling system experimentally. Luo et al. [17] conducted experimental study on the influence of operating parameters on dehumidification efficiency. Liu et al. [18]

compared the dehumidification efficiency of three different internally-cooled dehumidifiers and found that the dehumidifier with fin-coil structure was better than other dehumidifiers.

Surface material is one of the critical factors to dehumidification performance in internally-cooled falling film dehumidifiers. Falling film distribution on plate surface is heavily affected by surface properties, and the heat transfer between liquid desiccant and cooling fluid is also influenced by the heat conductivity of working plates. Therefore, metal plates are widely used in internally cooled falling film dehumidifiers. Yin et al. [20] developed a plate-fin heat exchanger using stainless steel material and investigated the dehumidification/regeneration performance. Dong et al. [21] proposed a new method to improve the dehumidification efficiency by utilizing TiO_2 superhydrophilic coating on stainless steel plate. In addition, plastic plates are also used in plate dehumidifiers due to good corrosion resistance and low cost. Kessling et al. [22] built a new parallel plate dehumidifier made of polypropylene double plates and investigated the dehumidification performance both experimentally and theoretically. Saman and Alizadeh [23] developed a plate heat exchanger using thin plastic plates for dehumidification/cooling and investigated the thermal and dehumidification behaviour experimentally and numerically. Liu et al. [24] designed a liquid desiccant dehumidifier with thermally-conductive plastic. The experimental results indicated that the plastic dehumidifier demonstrated comparable dehumidification performance compared with the metal dehumidifiers. Therefore, it is important to analyse the influence of plate surface properties on dehumidification performance.

To investigate the effect of surface properties on heat/mass transfer performance in falling film dehumidifiers, three commonly-used plate dehumidifiers, i.e., Stainless plate dehumidifier, Titanium plate dehumidifier and Polytetrafluoroethylene (PTFE) plate dehumidifier, with distinctive surface properties were investigated in this paper. Firstly, the surface free energy of different plate surfaces was measured to describe the adhesion between liquid desiccant and solid surface. To identify the principles of different surface properties, the microstructures of different plate surfaces were tested using SEM test. Then, an experimental setup of single-channel internally-cooled falling film dehumidifier with substitutable working plates was fabricated. The effect of surface properties on flow and heat/mass transfer performance was comprehensively investigated under various operating conditions. The flow characteristics of desiccant solution in terms of wetting area and falling film thickness were measured and analysed. Besides, the influencing factors of dehumidification performance, i.e., solution velocities and temperature, air velocities, temperature and air humidity as well as cooling water temperature were discussed. A novel empirical correlation of mass transfer coefficient was established considering the effect of surface properties on dehumidification performance through surface free energy. Finally, the electricity consumption of solar-

assisted air-conditioning system was simulated and the results indicated that improving surface wettability of falling film dehumidifier could reduce the electricity consumption effectively.

2. Experimental apparatus and performance index

2.1 Experimental apparatus

An experimental setup of the internally-cooled falling film dehumidifier with substitutable working plates was developed to analyse the influence of surface properties on dehumidification capacity. Fig. 2 and Fig. 3 show the schematic diagram and picture of the experimental setup which mainly consists of three sub-systems, i.e., air supply system (green line), liquid desiccant supply system (red line) and cooling water system (blue line). The sizes of the falling film plate dehumidifier and working plates are $550\times50\times600$ mm ($L\times W\times H$) and 550×600 mm ($L\times H$), respectively. The air was supplied by fans and then heated and humidified by an air heater and a humidifier. After being adjusted to the required experimental conditions, the air was provided to the falling film dehumidifier and interacted with the desiccant solution. Finally, the dry air flowed out at the top of the dehumidifier. The moisture of humid air was removed by desiccant solution due to vapor pressure difference between desiccant solution and humid air. The weak solution was then collected and regenerated in the regeneration system driven by solar energy. The inlet and outlet temperatures, density and flow rate of liquid desiccant were measured simultaneously in the experiment. Besides, the phase-change heat, released in absorption process, might increase the solution temperature and deteriorate the dehumidification performance. Therefore, an internally cooling unit was fixed in the experiment to take away the phase-change heat. In addition, ⑤ in Fig. 2 represents the working plate which is substitutable during the experiment. As contact area between processed air and desiccant solution was critical to dehumidification capacity, a thermal image camera was utilized in the experiment to record the shapes of the falling film and then to calculate the wetting area. Besides, the film thickness was measured by a capacitance micrometer. The specifications of the sensors, the thermal image camera and the capacitance micrometer are presented in Table 1.

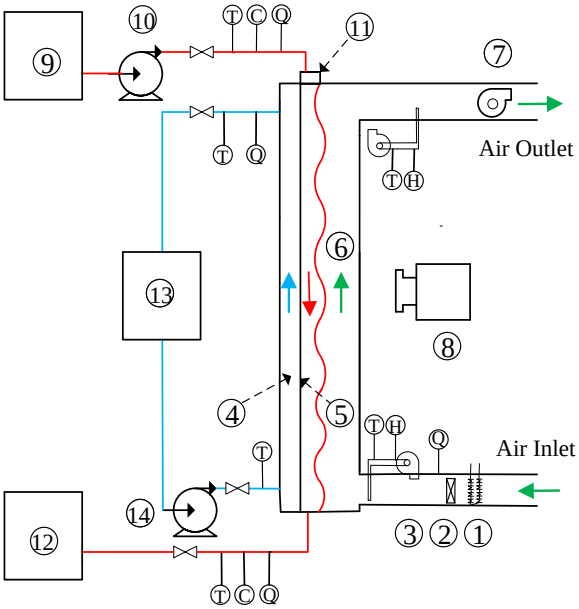

Ⓣ Temperature Sensor Ⓒ Density Sensor Ⓠ Flowmeter Ⓗ Wet-bulb temperature sensor

1、Air Heater 2、Humidifier 3、Sampling Fan 4、Internally Cooling Unit 5、Working Plate 6、Air Channle 7、Fan 8、Thermal Image Camera 9、Solution Provider Tank 10、Solution Pump 11、Solution distributor 12、Solution Collection Tank 13、Cooling Water Tank 14、Water Pump

Fig. 2 Schematic diagram of the experimental setup

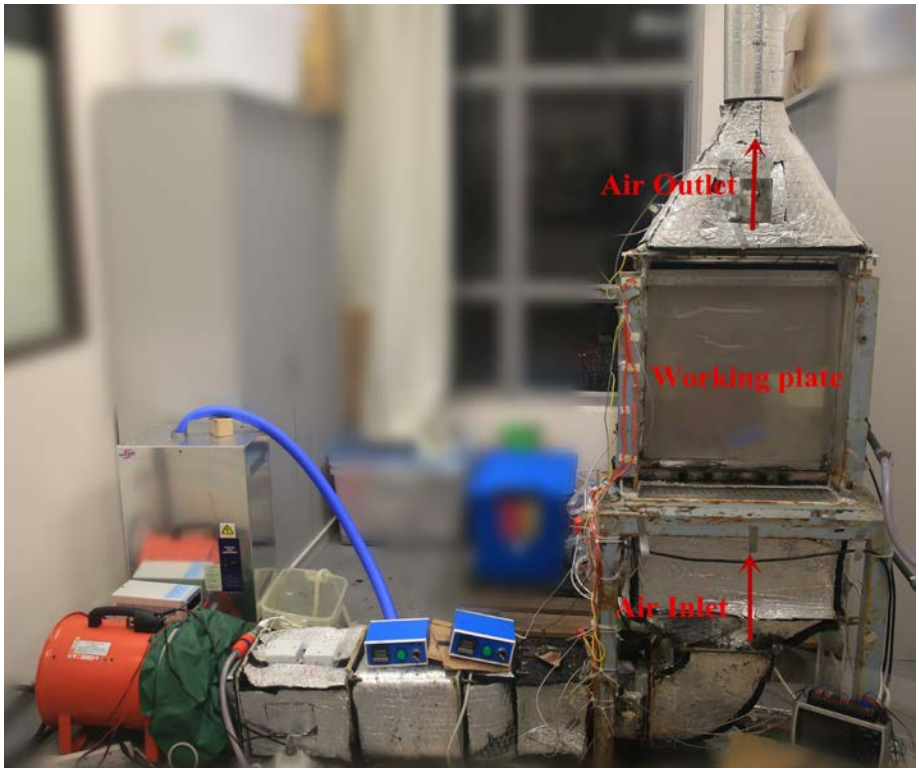

Fig. 3 Picture of the experimental setup

Table 1 Specifications of different measuring devices

Parameter	Device	Brand	Model	Accuracy	Operational range
Air/Solution/Cooling water temperature	Pt RTD	Heraeus	LN222-A	0.1 K	223-573 K
Air flow rate	Air velocity sensor	Shielur	ASF-100	0.3%	9-10000 Pa
Solution flow rate	Turbine flow rate sensor	Gems Sensors	173936-C	3%	0.5-5 L/min
Solution density	Specific gravity hydrometer	Daho	DH-300x	1 kg/m^3	1-99, 999 kg/m^3
Cooling water flow rate	Turbine flow rate sensor	Sea	YF-S201	2%	1-30 L/min
Falling film temperature	Thermal image camera	Fluke	Ti-200	2%	-20-650 ℃
Falling film thickness	Capacitance micrometer	-	JDC-2010	0.8 μm	0-1000 μm

2.2 Performance index

To better analyse the experimental results and compare the dehumidification performance between different plate dehumidifiers, three dehumidification performance indices, i.e., mass transfer coefficient, h_{D}, dehumidification efficiency, η_{ω}, and moisture removal rate, m_{ω}, were proposed in this paper. The definitions of these performance indices are shown as follows.

The mass transfer coefficient, h_{D}, represents the absorption rate of moisture at unit contact area.

$$h_{\mathrm{D}} = \frac{m_{\mathrm{a}}(\omega_{\mathrm{a,in}} - \omega_{\mathrm{a,out}})}{A\Delta\omega} \tag{1}$$

where m_{a} represents mass flow rates of processed air. $\omega_{\mathrm{a,in}}$ and $\omega_{\mathrm{a,out}}$ stand for absolute air humidity at inlet and outlet positions, respectively. A is the actual contact area between processed air and desiccant solution. $\Delta\omega$ represents the logarithmic mean humidity difference between liquid desiccant and processed air [24]. For counter-current falling film dehumidifier, $\Delta\omega$ can be expressed as follows.

$$\Delta\omega = \frac{\left(\omega_{\mathrm{a,in}} - \omega_{\mathrm{equ,out}}\right) - \left(\omega_{\mathrm{a,out}} - \omega_{\mathrm{equ,in}}\right)}{\ln \dfrac{\omega_{\mathrm{a,in}} - \omega_{\mathrm{equ,out}}}{\omega_{\mathrm{a,out}} - \omega_{\mathrm{equ,in}}}} \tag{2}$$

where ω_{equ} is the equilibrium humidity. The subscript of in and out mean inlet and outlet, respectively.

The dehumidification efficiency, η_{ω}, represents ratio of practical dehumidification performance to the maximum potential value.

$$\eta_{\omega} = \frac{\omega_{a,in} - \omega_{a,out}}{\omega_{a,in} - \omega_{equ,in}} \tag{3}$$

The moisture removal rate, m_{ω}, represents the dehumidification capacity of the dehumidifier at unit time, g/s.

$$m_{\omega} = m_a(\omega_{a,in} - \omega_{a,out}) \tag{4}$$

Besides, the uncertainty analysis is conducted in this study to better understand the experimental results. The detailed process of the uncertainty analysis can be referenced from Dong et al. [21]. Through the analysis, the uncertainty of the mass transfer coefficient, dehumidification efficiency and moisture removal rate are 5.4%, 3.4% and 3.2%, respectively.

3. Characterization of falling film dehumidifiers with distinctive surface properties

To investigate the effect of surface properties on heat/mass transfer performance for falling film dehumidifiers, three commonly-used plate dehumidifiers, i.e., Stainless plate dehumidifier, Titanium plate dehumidifier and Polytetrafluoroethylene (PTFE) plate dehumidifier, with distinctive surface properties were investigated.

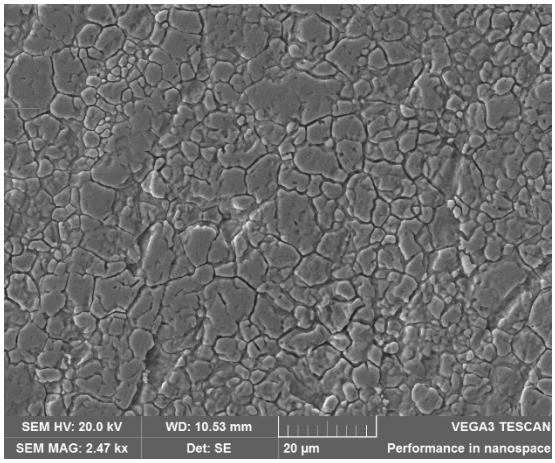

(a) Stainless steel plate surface

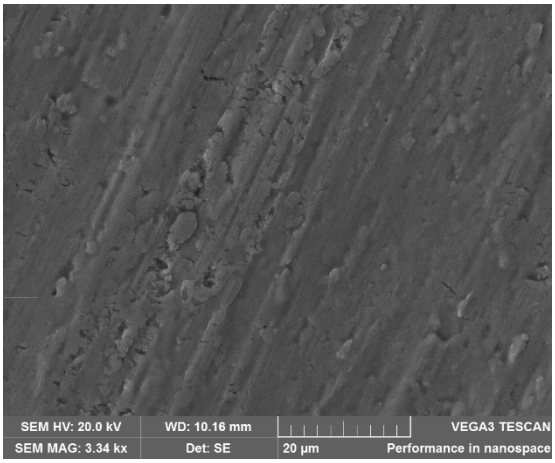

(b) Titanium plate surface

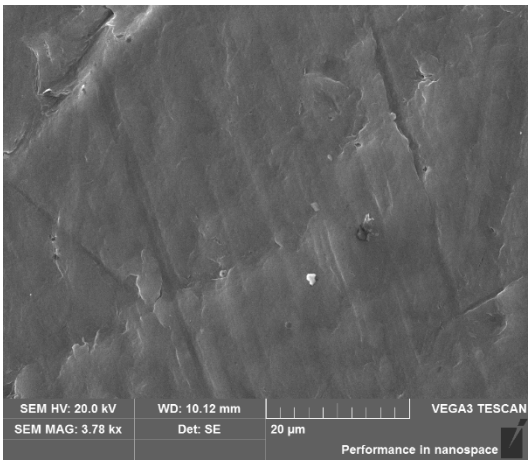

(c) PTFE plate surface

Fig. 4 SEM images of plate surfaces for different falling film dehumidifiers

As the wettability behaviour of solid surface is mainly governed by both chemical composition and geometric structures, SEM test was conducted to investigate the microstructures of plate surfaces with distinctive surface properties. As shown in Fig. 4(b), the Titanium plate surface demonstrates striate microstructures. Besides, secondary structure is also presented on the striate microstructures, which could enhance the capillarity and improve the surface wettability. As shown in Fig. 4(c), the PTFE plate surface shows smooth surface structure. This kind of surface morphology as well as the strong inter molecular bond between Fluoride and Carbon atoms result in the hydrophobicity of PTFE surface. The Stainless steel plate surface demonstrates cracked structures, as shown in Fig. 4(a), which results the medium surface wettability between Titanium and PTFE plate surfaces.

The wetting area of desiccant solution is one of the key parameters influencing dehumidification efficiency. In falling film desiccant dehumidifier, the wetting area under certain flow conditions is determined by surface wettability. Therefore, contact angle and surface free energy were introduced in this paper to study the surface wettability. The surface free energy was estimated based on contact angles using Owens-Wendt approach [25, 26]. In Owens-Wendt approach, surface free energy is assumed to be composed of polar and dispersive components. Owens-Wendt geometric average equation is shown as follows.

$$\gamma_L(1+\cos\theta) = 2(\gamma_S^D\gamma_L^D)^{1/2} + 2(\gamma_S^P\gamma_L^P)^{1/2} \quad (5)$$

where γ_L and γ_S represent liquid and solid surface free energy, respectively. The superscripts of P and D represent polar and dispersive component of surface free energy. θ is the contact angles of liquid on solid surface. To estimate solid surface free energy, at least two liquid regents with known surface free energy are necessary. Diiodomethane and deionized water were adopted to calculate the surface free energy in this study. The contact angles of diiodomethane and deionized water on different plate surfaces were tested at least five times by a Contact Angle meter using sessile drop method. The detailed contact angles and the pictures of liquid droplets on plate surfaces are presented in Table 2 and Fig. 5. The contact angles of diiodomethane and deionized on Titanium plate surface were much smaller than that on Stainless plate surface and PTFE plate surface, indicating that Titanium plate surface demonstrated superior surface wettability compared with the other plate surfaces. The data of contact angles were adopted to calculate the surface free energy of different plate surfaces using Owens-Wendt approach.

Table 2 Contact angles of diiodomethane and deionized water on plate surfaces with distinctive surface properties [°]

Samples		1	2	3	4	5	Average	Standard deviation
Titanium surface	Deionized water	52.3	54.5	51.5	54.0	55.2	53.3	1.32
	Diiodomethane	38.8	42.2	39.5	41.2	39.8	40.3	1.37
Stainless surface	Deionized water	85.4	85.0	89.5	88.2	89.4	87.5	2.16
	Diiodomethane	48.8	52.2	51.2	52.0	48.8	50.6	1.68
PTFE surface	Deionized water	112.0	109.5	113.0	109	107	110.1	2.41
	Diiodomethane	60.0	58.1	63.5	60.8	59.6	60.4	1.99

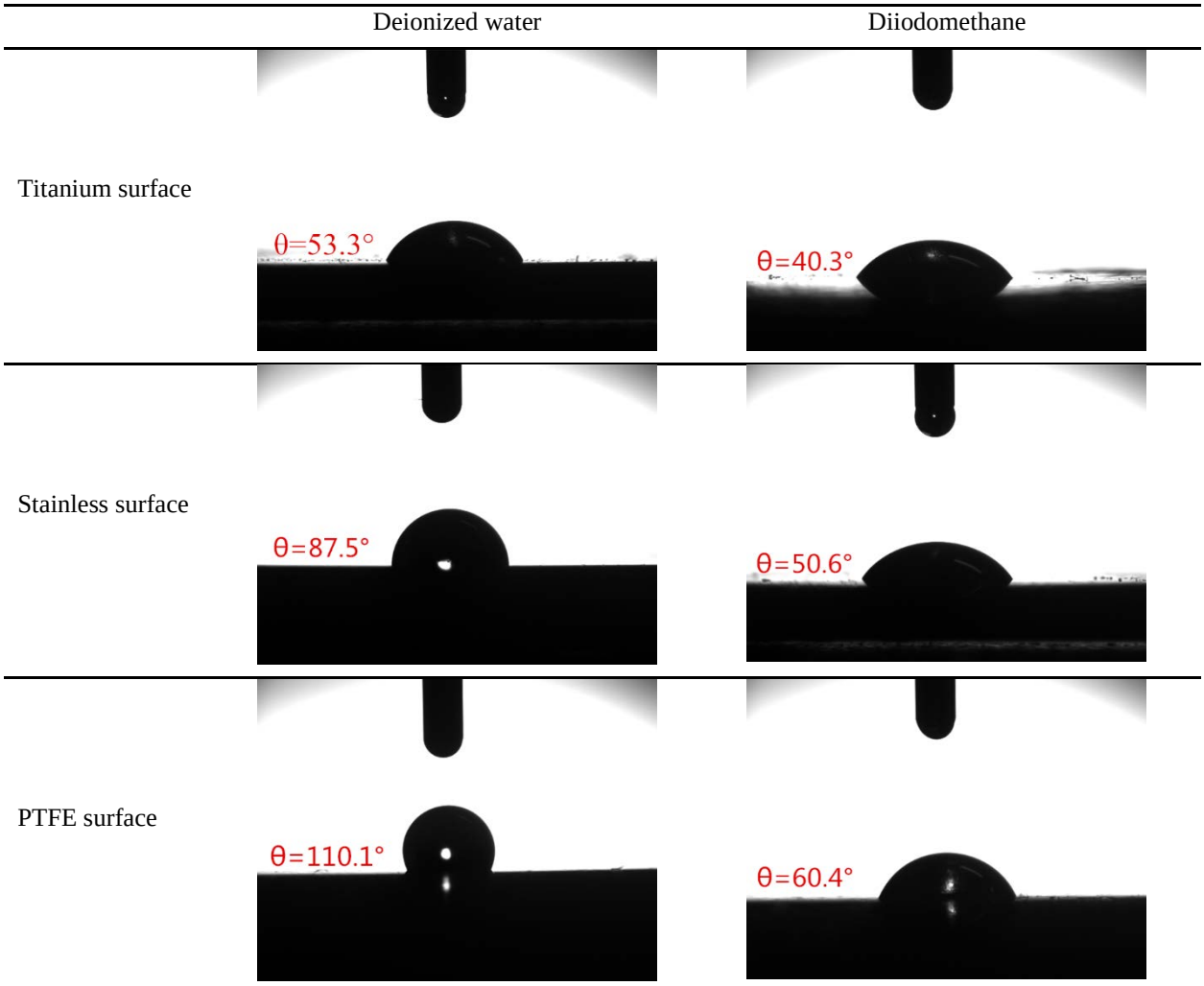

Fig. 5 Contact angles of diiodomethane and deionized water on plate surfaces with distinctive surface properties

Surface free energy is used to evaluate the surface wettability due to its independence from liquid reagents involved in the test. As surface free energy represents adhesion between liquid and solid surface, higher surface free energy means higher wetting ability. Table 3 shows the surface free energy of different plate surfaces calculated based on the contact angels of deionized water and diiodomethane using Owens-Wendt approach.

Titanium surface showed the highest surface free energy, indicating that Titanium plate surface was most hydrophilic amongst these three different plates. As the dispersive component of PTFE plate surface was almost equal to zero, its low surface free energy meant strong repellence between liquid and solid surface. Besides, the wettability difference of different plate surfaces will be shown below in terms of wetting area.

Table 3 Surface free energy of plate surfaces with distinctive surface properties

	Dispersive components γ_S^D (mJ/m^2)	Polar components γ_S^P (mJ/m^2)	Surface free energy γ_S (mJ/m^2)
Titanium plate	29.45	21.16	50.61
Stainless plate	33.83	3.15	36.98
PTFE plate	30.28	0.06	30.34

Besides, the thermal properties of the working plates are also important to dehumidification performance, especially in internally-cooled falling film dehumidifiers. Table 4 presents the physical properties, i.e., thermal conductivity, melting point and extension strength, of plate surfaces for different falling film dehumidifiers.

Table 4 Physical properties of plate surfaces with distinctive surface properties

	Thermal conductivity W/(m·K)	Temperature interval (℃)	Extension strength (MPa)
Titanium plate	15.24	1725 (melting point)	370-530
Stainless plate	16.3	1500 (melting point)	>520
PTFE plate	0.25	<250	22.0-35.0

4. Results and discussion

To compare the dehumidification capability and analyse the influence of surface properties on dehumidification capacity, more than 50 experimental conditions for each plate dehumidifier were conducted. Table 5 shows the ranges of experimental parameters and Table 6 shows part of the experimental results in detail.

Table 5 Ranges of experimental parameters

$T_{a,in}$ (℃)	$\omega_{a,in}$ (g/kg)	$m_{a,in}$ (kg/s)	$T_{s,in}$ (℃)	$m_{s,in}$ (kg/s)	$T_{f,in}$ (℃)
28.3-40.2	13.9-24.6	0.028-0.079	18.1-30.2	0.015-0.046	16.6-25.9

Table 6 Part of the detailed experimental results in different plate dehumidifiers

No.	$T_{a,in}$ (℃)	$T_{a,out}$ (℃)	$\omega_{a,in}$ (g/kg)	$\omega_{a,out}$ (g/kg)	$T_{s,in}$ (℃)	$T_{s,out}$ (℃)	$T_{f,in}$ (℃)	$T_{f,out}$ (℃)	m_a (kg/s)	m_s (kg/s)
1	30.7	27.0	21.4	17.5	24.5	25.3	16.2	17.7	0.061	0.046
2	35.8	30.2	21.6	18.1	24.4	25.3	16.3	17.8	0.060	0.047
3	29.8	26.8	17.5	15.1	24.9	25.3	16.3	17.4	0.062	0.048
4	30.3	27.9	21.6	17.4	25.2	25.8	16.8	18.8	0.061	0.048
5	30.6	28.8	21.1	17.5	27.3	28.3	16.7	18.1	0.069	0.046
6	30.5	28.3	21.3	17.4	26.0	26.6	16.9	18.1	0.050	0.046
7	30.7	28.0	21.8	18.3	24.4	26.4	17.4	18.6	0.062	0.028
8	30.8	28.7	21.8	18..6	25.1	28.6	16.5	17.8	0.062	0.016
9	30.9	29.3	22.2	19.1	27.0	27.6	24.2	25.2	0.061	0.047
10	29.5	27.8	21.3	18.3	30.1	30.4	16.7	17.8	0.061	0.046

To make the experimental results reliable and reduce the random errors, the replicate test was conducted. The experiment under each experimental condition was conducted four times and each test would last for at least 10 minutes under steady state. The experimental results indicated that all of the experimental results fell within $\pm$10% error of the mean values and the mean relative standard deviation was 4.1%.

The energy conservation analysis is also necessary to validate the experimental results. During the experiment, the energy released by processed air should be equal to that absorbed by desiccant solution and cooling water, which is given as follows.

$$m_a(h_{a,in}-h_{a,out})=(m_{s,out}h_{s,out}-m_{s,in}h_{s,in})+m_f C_{p,f}(T_{f,out}-T_{f,in}) \tag{6}$$

where m_a, m_s and m_f represent mass flow rates of processed air, solution and cooling fluid, respectively. h_a and h_s are enthalpy of processed air and liquid desiccant. T_f means the cooling water temperature. Besides, the subscript, in and out, represent the inlet and outlet of the falling film dehumidifier.

Average relative deviation (ARD) represent the discrepancies between the energy released from air side and the energy absorbed by desiccant solution and cooling water side.

$$\text{ARD}=\frac{1}{n}\sum_{i=1}^{n}\frac{E_a-(E_s+E_f)}{E_a} \tag{7}$$

where E_a represents the energy released by air side. E_s and E_f represent the energy absorbed by desiccant solution and cooling water side. *n* is the number of experimental data.

The energy conservation analysis between processed air, solution and cooling fluid are shown in Fig. 6. The discrepancies are within ±30 % with the average relative deviation (ARD) of 4.3%, which validates the reliability of the experimental results.

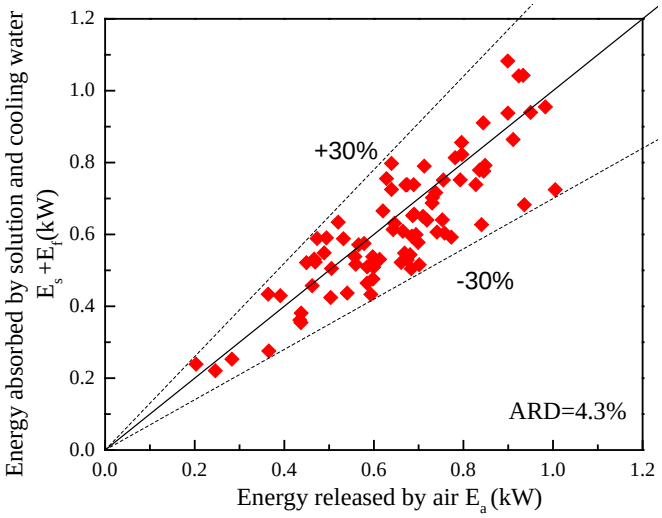

Fig. 6 Energy conservation of air, liquid desiccant and cooling water

4.1 Wetting area and film thickness

Wetting area of desiccant solution is an important parameter influencing dehumidification capacity. In this study, the wetting area was captured by a thermal image camera. Fig. 7 presents the thermal images of desiccant solution film in different falling film dehumidifiers with distinctive surface properties. The experimental results proved that surface wettability demonstrate positive effect on wetting area. In falling film dehumidifier with poor surface wettability (PTFE plate dehumidifier), the falling film of desiccant solution shrank rapidly along the flow direction. The initial wetting length of falling film at the inlet was 45 cm, but it was reduced rapidly to only 16 cm at the outlet, reducing the contact area between solution and humid air significantly. However, the falling film of desiccant solution shrank little in falling film dehumidifier with better surface wettability (Titanium plate dehumidifier) due to higher surface free energy.

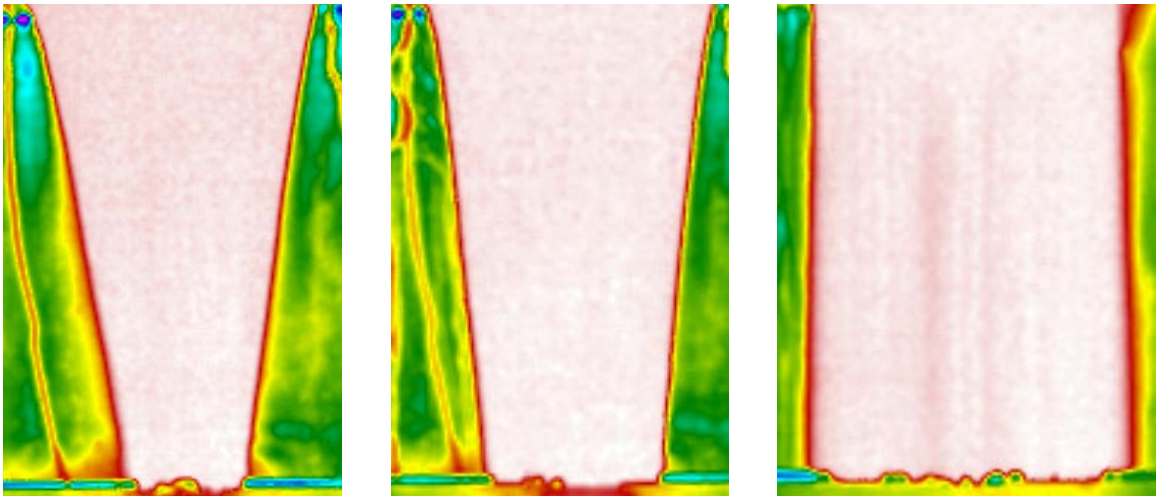

(a) PTFE plate dehumidifier (b) Stainless steel plate dehumidifier (c) Titanium plate dehumidifier

Fig. 7 Thermal images of desiccant solution film in different plate dehumidifiers

($m_{s,in}$ =0.047 kg/s, $T_{s,in}$ =24.6℃)

Fig. 8 shows the effect of solution flow rates on wetting area of falling film in different plate dehumidifiers. Wetting ratio, φ_A , the ratio of actual wetting area to the whole area, is introduced to describe the wetting conditions of falling film in plate dehumidifiers with different surface properties. The experimental results indicated that the wetting ratios increased rapidly with solution flow rates, especially in the plate dehumidifier with poor surface wettability (PTFE plate dehumidifier). The surface wettability demonstrated positive effect on the wetting conditions of falling film. The wetting area in plate dehumidifier with high surface wettability (Titanium plate dehumidifier) is much larger than that in the falling dehumidifier with poor surface wettability (PTFE plate dehumidifier). The maximum wetting ratio increased from 68.5% in PTFE plate dehumidifier to 98.4% in Titanium plate dehumidifier due to the better surface wettability of Titanium plate surface.

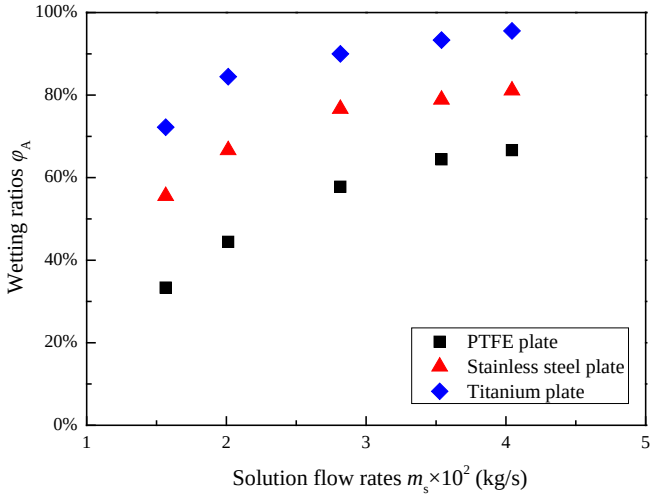

Fig. 8 Effect of solution flow rates on wetting ratios in different plate dehumidifiers

The average falling film thickness of desiccant solution was measured in the experiment using a capacitance micrometer to investigate the effect of surface properties on flow characteristics of liquid desiccant. Fig. 9 presents the variation of film thickness with desiccant solution flow rates in different falling film dehumidifiers. The experimental results indicated that improving surface wettability could reduce the falling film thickness effectively. In falling dehumidifier with poor surface wettability (PTFE plate dehumidifier), the falling film thickness ranged from 490 μm to 730 μm with Re_L increasing from 19.3 to 104.2, while it ranged from 450 μm to 592 μm in plate dehumidifier with higher surface wettability (Titanium plate dehumidifier). Besides, the heat transfer resistance between surface liquid desiccant and cold fluid was improved in falling film dehumidifier with poor surface wettability due to the thick falling film thickness and the dehumidification performance was deteriorated accordingly. Besides, the low thermal conductivity of PTFE plate dehumidifier also prevented the timely removal of latent heat by cooling water and deteriorated the dehumidification performance accordingly.

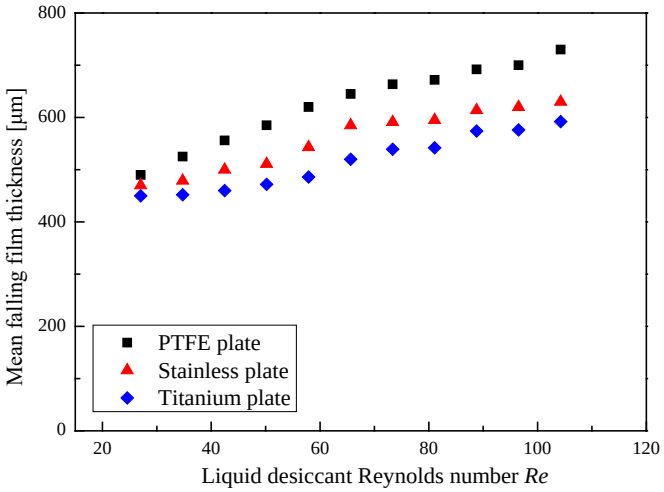

Fig. 9 Average film thickness with Reynolds number on different working plates

4.2 Dehumidification performance analysis

Under the experimental conditions presented in Table 7, the effect of surface properties on dehumidification performance are investigated. Fig. 10 presents the dehumidification performance of three different falling film dehumidifiers with distinctive surface properties. The experimental results proved that the surface wettability contributed positively in dehumidification performance. As the surface free energy increased from 30.34 mJ/m^2 (PTFE plate dehumidifier) to 50.61 mJ/m^2 (Titanium plate dehumidifier), the moisture removal rate increased from 0.155 to 0.213 with the enhancing ratio of 37.4% and dehumidification efficiency increased from 0.160 to 0.214 with the enhancing ratio of 33.8%, respectively. The performance enhancement is attributed to several reasons. Firstly, the wetting area on Titanium plate dehumidifier is largest due to the strong adhesion between liquid desiccant and solid surface with high surface wettability, as shown in Fig. 10, which contributes significantly to the dehumidification performance. Secondly, the falling film thickness in Titanium plate dehumidifier is the smallest due to the smooth disperse of liquid desiccant over plate surfaces, which could also contribute to the dehumidification performance enhancement. Besides, the heat conductivity of Titanium plate is much larger than that of PTFE plate and the latent heat is easily removed by cold water in Titanium plate dehumidifier.

Table 7 Experimental conditions of different falling film dehumidifiers

$T_{a,in}$ (℃)	$\omega_{a,in}$ (g/kg)	$m_{a,in}$ (kg/s)	$T_{s,in}$ (℃)	$m_{s,in}$ (kg/s)	$T_{f,in}$ (℃)
36	21.0	0.061	24.6	0.047	16.5

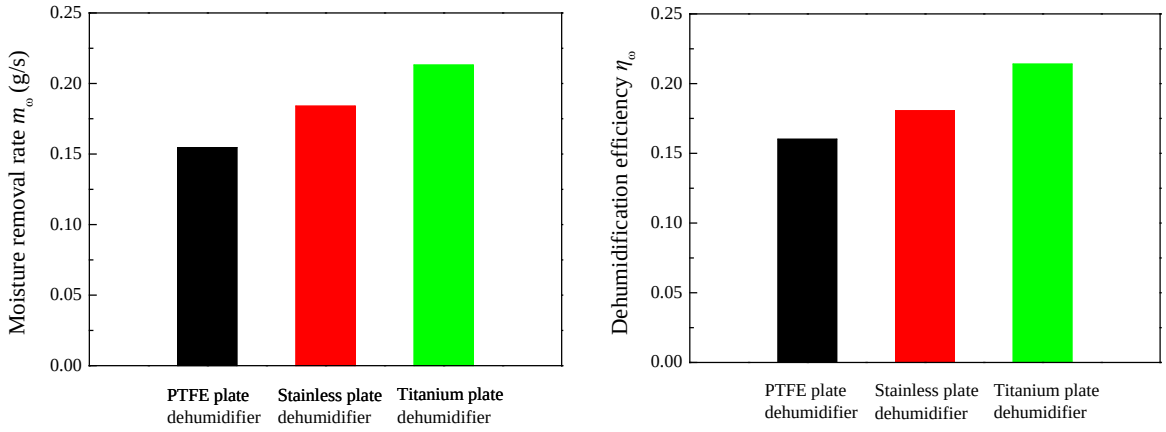

(a) Moisture removal rate m_ω (b) Dehumidification efficiency η_ω

Fig. 10 Comparison of dehumidification performance in plate dehumidifiers with distinctive surface properties

4.3 Influencing factors analysis

To analyses the dehumidification characteristics of falling film dehumidifiers with different surface properties, controlling variable method (CVM) was adopted in the experiment. The influence of flow parameters on dehumidification capacity in falling film dehumidifiers with distinctive surface properties was investigated comprehensively.

4.3.1 Influence of air flow rates

Fig. 11 presents the variation of dehumidification capacity with air flow rates in falling film dehumidifiers with different surface properties. The experimental conditions are shown in Table 8. The improvement of the moisture removal rate is explained by concentration polarization theory. The vapor moisture within boundary layer of processed air was depleted during dehumidification process and the driving force between processed air and liquid desiccant was reduced due to concentration polarization. Increasing air velocity can attenuate the boundary layer and lower the concentration polarization. Besides, the dehumidification performance difference between falling film dehumidifiers with different surface properties became larger with higher air flow rate. As the air flow rate increased from 2.89×10^{-2} kg/s to 7.85×10^{-2} m/s, the enhancing ratio between Titanium plate dehumidifier and PTFE plate dehumidifier increased from 17.7% to 56.3%, indicating that the falling film dehumidifier with better surface wettability could achieve higher moisture handling capacity at higher air velocities.

Table 8 Dehumidification experimental conditions with different air flow rates

$T_{a,in}$ (℃)	$\omega_{a,in}$ (g/kg)	$m_{a,in}$ (kg/s)	$T_{s,in}$ (℃)	$m_{s,in}$ (kg/s)	$T_{f,in}$ (℃)
30.3	21.1	0.028-0.078	25.5	0.047	16.8

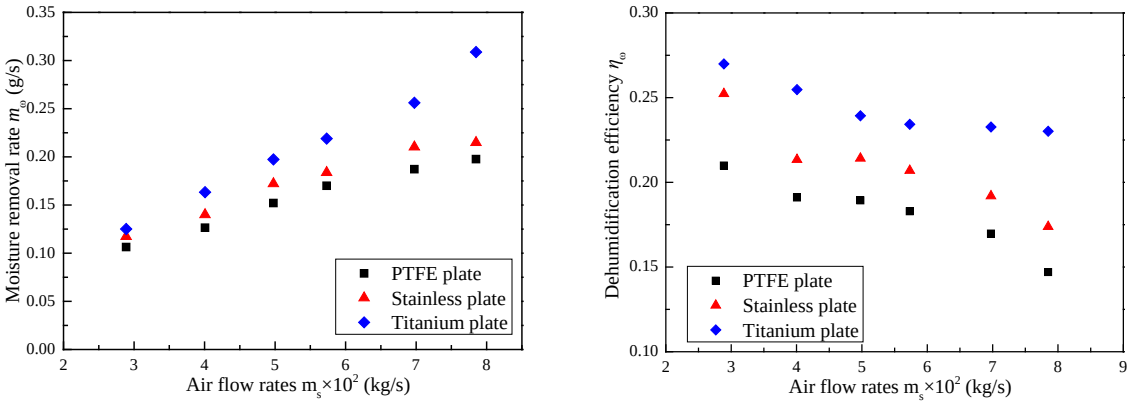

(a) Moisture removal rate m_ω (b) Dehumidification efficiency η_ω

Fig. 11 Influence of air flow rates on dehumidification capacity in different plate dehumidifiers.

4.3.2 Influence of air temperature

Fig. 12 shows the influence of air temperature on dehumidification performance for falling film dehumidifiers with distinctive surface properties. The experimental conditions are shown in Table 9. The air temperature presented negative influence on dehumidification capacity. As the air temperature increased from 28.3 ℃ to 40.2 ℃, the moisture removal rate decreased from 0.262 g/s to 0.197 g/s and the dehumidification efficiency from 0.253 to 0.190 for falling film dehumidifier with better surface wettability (Titanium plate dehumidifier). The negative influence of air temperature on dehumidification capacity resulted from the fact that the solution was heated by hot air during dehumidification process. As the equilibrium pressure above desiccant solution increased with solution temperature, the driving force of dehumidification process between processed air and liquid desiccant was reduced. Besides, the difference of dehumidification performance for falling film dehumidifiers with different surface properties varied little with air temperature, indicating that the air temperature demonstrated the same effect on dehumidifiers with different surface properties.

Table 9 Dehumidification experimental conditions with different air temperature

$T_{a,in}$ (℃)	$\omega_{a,in}$ (g/kg)	$m_{a,in}$ (kg/s)	$T_{s,in}$ (℃)	$m_{s,in}$ (kg/s)	$T_{f,in}$ (℃)
28.3-40.2	21.0	0.061	24.6	0.047	16.5

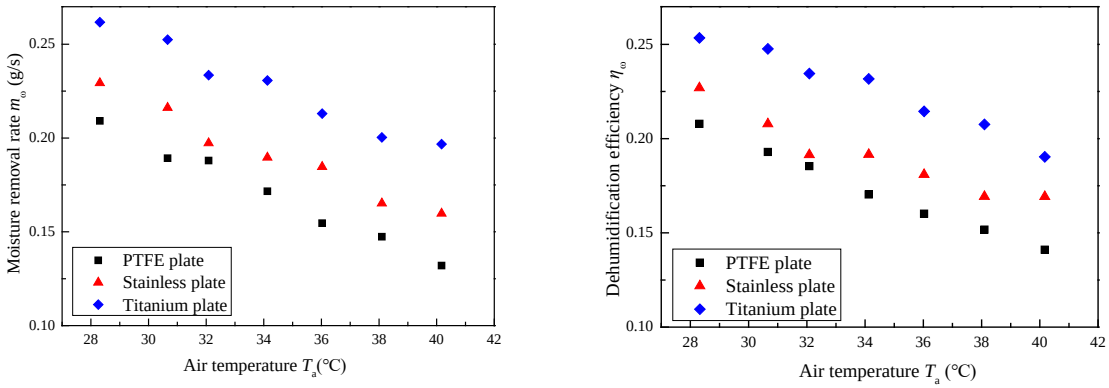

(a) Moisture removal rate m_ω (b) Dehumidification efficiency η_ω

Fig. 12 Influence of air temperature on dehumidification capacity in different plate dehumidifiers.

4.3.3 Influence of air humidity

Fig. 13 presents the variation of dehumidification capacity with air humidity. This set of experiment were conducted under the conditions shown in Table 10. The moisture removal rate increased linearly with air humidity due to the humidity difference between processed air and desiccant solution. As the air humidity increased from 13.9 g/kg to 24.6 g/kg, the moisture removal rate increased from 0.099 g/s to 0.316 g/s with the enhancing ratio of 219% in Titanium plate dehumidifier. Besides, the dehumidification performance difference between falling film dehumidifiers with different surface properties becomes less obvious at higher air humidity. The condensation of water vapor might occur on the unwetted plate surface under high humidity condition, which might increase the dehumidification performance of falling film dehumidifier with poor surface wettability and reduce the difference of dehumidification performance.

Table 10 Dehumidification experimental conditions with different air humidity

$T_{a,in}$ (℃)	$\omega_{a,in}$ (g/kg)	$m_{a,in}$ (kg/s)	$T_{s,in}$ (℃)	$m_{s,in}$ (kg/s)	$T_{f,in}$ (℃)
30.2	13.9-24.6	0.062	25.2	0.047	16.4

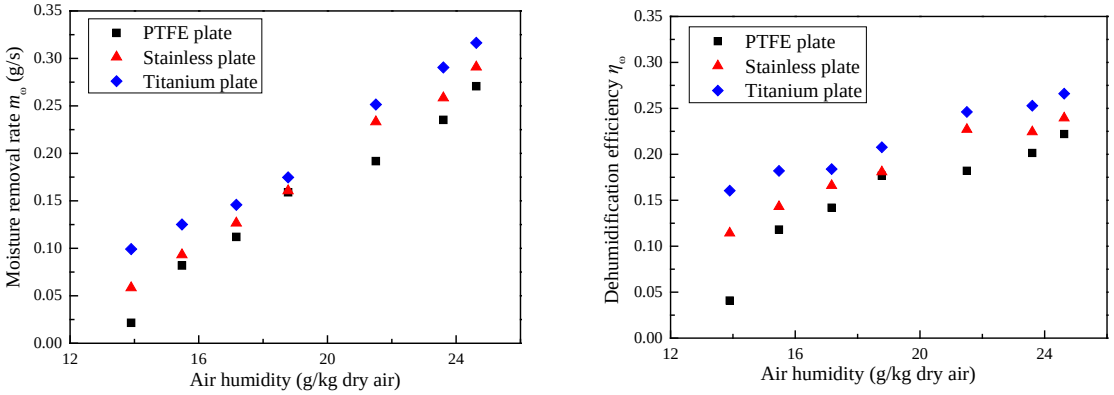

(a) Moisture removal rate m_ω (b) Dehumidification efficiency η_ω

Fig. 13 Influence of air humidity on dehumidification capacity in different plate dehumidifiers

4.3.4 Influence of desiccant solution temperature

The water vapor exchange is driven by the pressure difference between desiccant solution and humid air. Therefore, the equilibrium pressure of desiccant solution, mainly determined by solution temperature and concentration, is critical to dehumidification capacity. Fig. 14 presents the influence of desiccant solution temperature on dehumidification capacity. The experimental conditions are presented in Table 11. The dehumidification capacity dropped with increase of desiccant solution temperature, which resulted from the increase of equilibrium pressure by higher solution temperature. In Fig. 14(a), the dehumidification performance difference between different plate dehumidifiers decreased with solution temperature. As the solution temperature increased from 18.8 ℃ to 30.0 ℃, the dehumidification difference between Titanium and PTFE plate dehumidifiers decreased from 0.0564 g/s to 0.0315 g/s. According to Qi et al. [27], the falling film shrinkage was deteriorated at higher solution temperature. Therefore, the difference in wetting area between different falling film dehumidifiers with distinctive surface properties was reduced with solution temperature and the dehumidification performance difference was narrowed accordingly.

Table 11 Dehumidification experimental conditions with different solution temperature

$T_{a,in}$ (℃)	$\omega_{a,in}$ (g/kg)	$m_{a,in}$ (kg/s)	$T_{s,in}$ (℃)	$m_{s,in}$ (kg/s)	$T_{f,in}$ (℃)
29.5	21.6	0.061	18.8-30	0.046	16.9

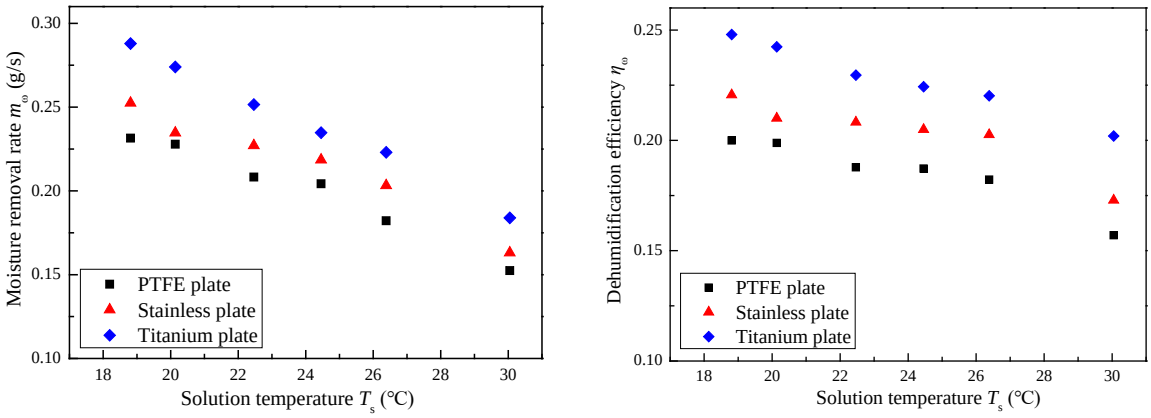

(a) Moisture removal rate m_ω (b) Dehumidification efficiency η_ω

Fig. 14 Influence of desiccant solution temperature on dehumidification capacity in different plate dehumidifiers

4.3.5 Influence of solution flow rates

Fig. 15 shows that the dehumidification capacity increases with desiccant solution flow rates under the experimental conditions presented in Table 12. The enhancement of dehumidification capacity by desiccant solution flow rates is ascribed to several factors. On one hand, the wetting area of desiccant solution increased with desiccant flow rates. On the other hand, the fluctuation of falling film was also enhanced by desiccant flow

rates, which could reduce the concentration polarization effect at the interface between desiccant solution and processed air.

Table 12 Dehumidification experimental conditions with different solution flow rates

$T_{a,in}$ (℃)	$\omega_{a,in}$ (g/kg)	$m_{a,in}$ (kg/s)	$T_{s,in}$ (℃)	$m_{s,in}$ (kg/s)	$T_{f,in}$ (℃)
30.4	21.8	0.062	25.8	0.015-0.041	16.6

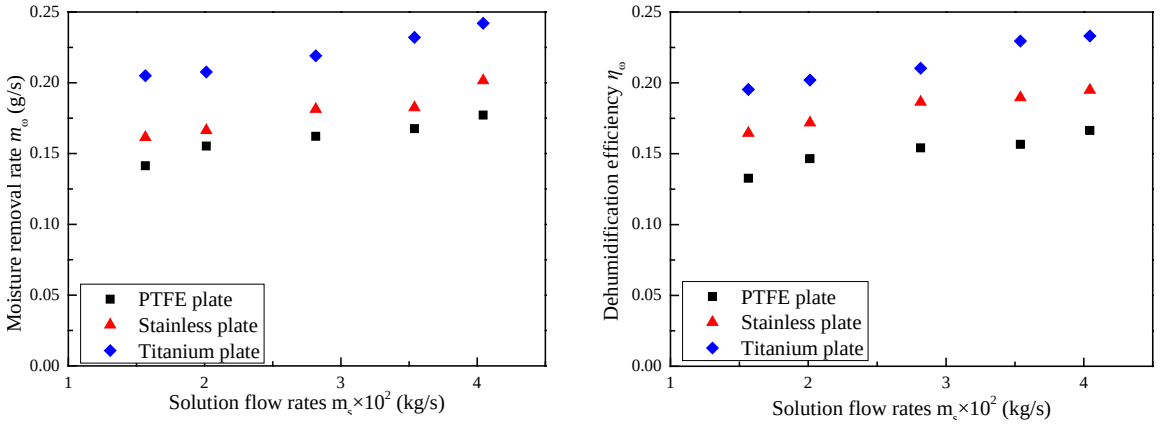

(a) Moisture removal rate m_ω (b) Dehumidification efficiency η_ω

Fig. 15 Influence of solution flow rates on dehumidification capacity in different plate dehumidifiers

4.3.6 Influence of cooling fluid temperature

As presented in Fig. 16, the dehumidification performance decreased slightly with cooling water temperature. The experimental conditions are shown in Table 13. The cooling fluid was used to remove the heat during the dehumidification process and maintain the solution temperature. As the cooling water temperature increases, the heat transfer between desiccant and cooling fluid was reduced, which resulted in temperature increase of desiccant solution and deteriorated the dehumidification performance accordingly. Besides, the dehumidification performance difference between falling film dehumidifiers with different surface properties decreased with cooling fluid temperature. As the cooling water temperature increased from 16.4 ℃ to 25.7 ℃, the dehumidification difference between Titanium and PTFE plate dehumidifiers decreased from 0.0555 g/s to 0.0340 g/s.

Table 13 Dehumidification experimental conditions with different cooling fluid temperature

$T_{a,in}$ (℃)	$\omega_{a,in}$ (g/kg)	$m_{a,in}$ (kg/s)	$T_{s,in}$ (℃)	$m_{s,in}$ (kg/s)	$T_{f,in}$ (℃)
30.9	21.6	0.062	26	0.046	16.6-25.9

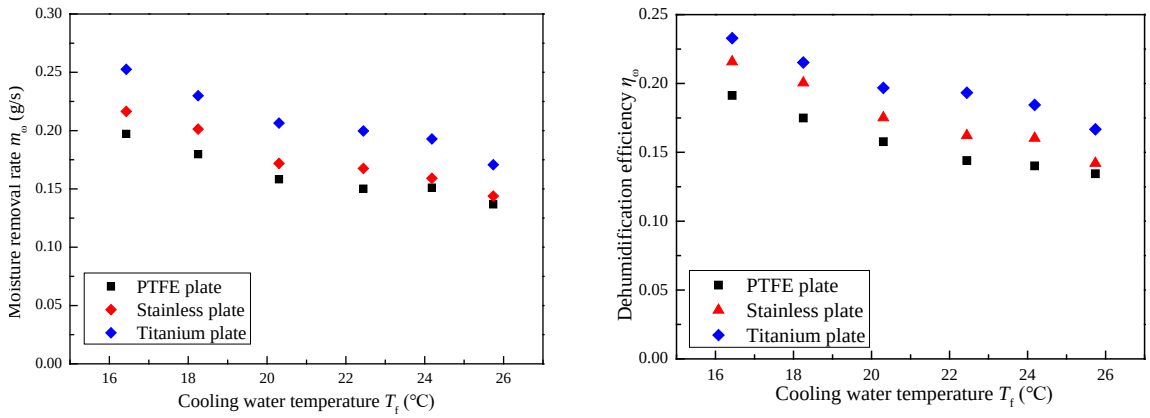

(a) Moisture removal rate m_ω (b) Dehumidification efficiency η_ω

Fig. 16 Influence of water temperature on dehumidification capacity in different plate dehumidifiers

4.4 Correlation development of mass transfer coefficient

In this study, the dehumidification capacity of falling film dehumidifiers with distinctive surface properties was investigated to analyse the effect of surface properties on dehumidification performance. The surface wettability of different plate dehumidifiers were tested and characterized by surface free energy. Besides, the effect of flow parameters on dehumidification capacity for falling film dehumidifiers with distinctive surface properties were comprehensively analysed. Therefore, a novel empirical correlation of mass transfer coefficient was established, within which surface free energy was considered to account for the effect of surface wettability on dehumidification performance. Based on the research by Liu et al. [24] and the analysis of influencing factors above, the original form of the mass transfer correlation was identified, as shown in Eq.(8).

$$h_D = \mathrm{k} f(\gamma) \times m_a^{a_1} \times m_s^{a_2} \times T_a^{a_3} \times T_s^{a_4} \times T_f^{a_5} \times \omega_a^{a_6} \tag{8}$$

where h_D is the mass transfer coefficient. m_a and m_s represent the mass flow rates of processed air and desiccant solution. T_a, T_s and T_f are the temperature of processed air, desiccant solution and cooling fluid, respectively. ω_a is the humidity of processed air. $f(\gamma)$ is a function of surface free energy, which accounts for the effect of surface wettability on dehumidification performance. To simplify the deviation process, the form of $f(\gamma)$ is expressed as follows.

$$f(\gamma) = b - c\gamma^{-d} \tag{9}$$

where γ represents surface free energy of plate surface. The exponents, k, a_1-a_6, b and c, in Eqs. (8) and (9) were identified based on the experimental results using non-linear regression method. Thus, the newly-developed mass transfer correlation was identified as follows.

$$h_D = 4.5\times10^{-4} \times f(\gamma) \times m_a^{0.88} \times m_s^{0.23} \times T_a^{-0.65} \times T_s^{-0.21} \times T_f^{-0.67} \times \omega_a^{1.12} \tag{10}$$

$$f(\gamma) = 1.29 \times 10^4 - 6.08\gamma^{-1.89} \tag{11}$$

Eq. (11) indicates that $f(\gamma)$ increases with surface free energy, which accords with the observation during the experiment. The effect of surface wettability on dehumidification performance could be effectively represented by $f(\gamma)$.

As shown in Fig. 17, the newly-developed correlation could accurately predict experimental results within ±10 %. The absolute relative deviation of the calculate results is 5.4 %, validating the newly-developed correlation.

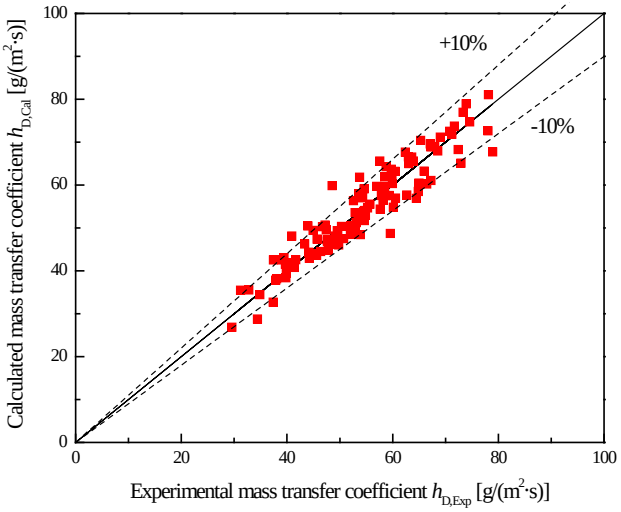

Fig. 17 Comparison between the calculated and experimental mass transfer coefficients

5. Energy consumption analysis of solar-assisted liquid desiccant air-conditioning system

To estimate the energy consumption of solar-assisted liquid desiccant air-conditioning system, a dynamic model composing of an internally-cold liquid desiccant dehumidifier, an internally-heated liquid desiccant regenerator, a solar collector and auxiliary heater, a cooling coil and several heat exchangers is developed, as shown in Fig. 18. To accurately identify parameters of the system, three iteration loops, i.e., iteration loop of liquid desiccant solution (blue line), iteration loop of heating water (red line) and iteration loop of cooling water (black line), are considered in the dynamic model.

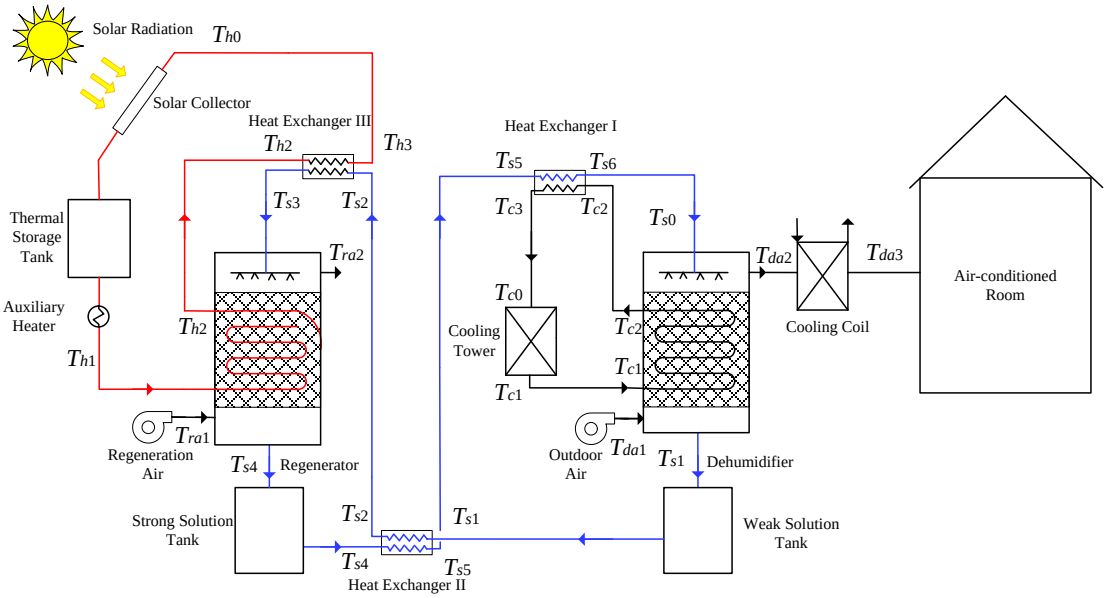

Fig. 18 Schematic diagram of solar-assisted air-conditioning system

The outlet parameters of each component are calculated based on the inlet parameters and operating efficiency. The specifications of the main components are presented in Table 14. A typical commercial building located in Hong Kong, composed of 2 floors of car-park (1600 m^2/floor), 3 floor of retail (1600 m^2/floor) and 24 floors of office (545 m^2/floor for 5-15/F and 515 m^2/floor for 16-26), is selected as the case building. The thermal properties of the building components, including windows, walls and roofs, are referenced from the energy code by the Hong Kong Government [28]. The detailed specifications of the building can be referenced in Qi et al. [29].

Table 14 Specifications of main devices

Dehumidifier/regenerator	Size	550×600 mm
Solar collector	Rated efficiency	0.84
	Angle	22.5°
Auxiliary electrical heater	Rated efficiency	0.90
Cooling coil	COP	3.3
Cooling tower	Rated efficiency	0.45
Heat exchanger	Rated efficiency	0.93 (I and III) 0.54 (II)
Air fan	Rated efficiency	0.70
Pump	Rated efficiency	0.65

Fig. 19 shows the annular electricity use of solar-assisted air-conditioning system using falling film dehumidifiers with distinctive surface properties. The results indicate that surface wettability presents positive influence on energy efficiency. The solar-assisted air-conditioning system with Titanium plate dehumidifiers demonstrates superior energy efficiency to that with the other plate dehumidifiers. Improving surface wettability

could reduce the energy consumption effectively. It is estimated that 9.6 % (130 MW·h) of the energy consumption could be saved for the air-conditioning system with Titanium plate dehumidifier compared to that with PTFE plate dehumidifiers. The lower energy consumption is attributed to higher dehumidification efficiency of falling film dehumidifier with better surface wettability.

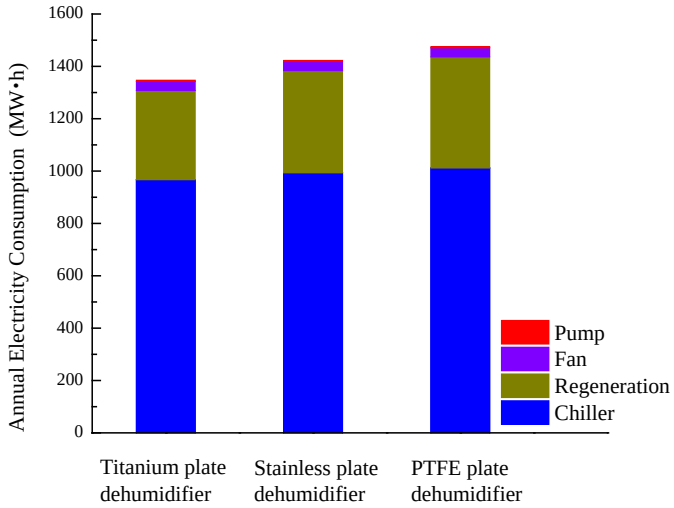

Fig. 19 Annular electricity consumption of solar-assisted liquid desiccant air-conditioning system with different working plates

6. Conclusions

The investigation on dehumidification capacity of internally-cold falling film dehumidifiers with distinctive surface properties were conducted comprehensively in this study. The main conclusions are summarized as follows.

(1) Three types of falling film dehumidifiers with distinctive surface properties was used to investigate the effect of surface properties on dehumidification performance. The surface free energy of Titanium plate surface, Stainless plate surface and PTFE plate surface were 50.61 mJ/m^2, 36.98 mJ/m^2 and 30.34 mJ/m^2, respectively, indicating that Titanium plate demonstrated the superior wettability compared with the other plates.

(2) The effect of surface properties on flow characteristics of falling film was investigated. Surface wettability demonstrated positive effect on wetting area of falling film. The falling film shrank seriously along the flow direction in falling film dehumidifier with poor surface wettability (PTFE plate dehumidifier) due to the strong repellence between liquid desiccant and solid surface, while it shrank little in falling film dehumidifier with better surface wettability (Titanium plate dehumidifier). Besides, the PTFE plate dehumidifier presented the thickest falling film which increased the heat transfer resistance inside the solution and deteriorated dehumidification capacity.

(3) The effect of surface wettability on dehumidification performance was comprehensively investigated. The surface wettability contributed positively to dehumidification performance. As the surface free energy increased from 30.34 mJ/m^2 (PTFE plate dehumidifier) to 50.61 mJ/m^2 (Titanium plate dehumidifier), the moisture removal rate increased from 0.155 to 0.213 with the enhancing ratio of 37.4% and dehumidification efficiency increased from 0.160 to 0.214 with the enhancing ratio of 33.8%, respectively.

(4) A novel empirical correlation of mass transfer coefficient was developed. The surface free energy was considered in the new correlation to account for the effect of surface wettability on dehumidification performance.

(5) The effect of surface properties on energy consumption for solar-assisted liquid desiccant air-conditioning system was investigated. Increasing surface wettability could reduce the energy consumption effectively. It is estimated that 9.6 % (130 MW·h) of the energy consumption could be saved for the air-conditioning system with Titanium plate dehumidifier compared to that with PTFE plate dehumidifier.

Improving surface wettability could enhance the heat/mass transfer performance of falling film dehumidifiers rapidly. This study provides an effective approach to improve operating performance of other falling film applications, such as evaporators, condensers and chemical columns.

Acknowledgements

This work was supported by the RGC General Research Fund (PolyU 152010/15E) and the RGC General Research Fund (PolyU 152184/17E).

References

[1] Kabeel AE. Dehumidification and humidification process of desiccant solution by air injection. Energy 2010;35(12):5192-5201.

[2] Fong KF, Lee CK. Impact of adsorbent characteristics on performance of solid desiccant wheel. Energy 2018;144:1003-1012.

[3] Hong Kong Energy End-Use Data. Electrical and Mechanical Services Department of Hong Kong Special Administrative Region, 2017.

[4] Waugaman DG, Kini A, Kettleborough CF. A review of desiccant cooling systems. Journal of Energy Resources Technology 1993;115(1):1-8.

[5] Miyara A, Onaka Y, Koyama S. Ways of next generation refrigerants and heat pump/refrigeration systems. International Journal of Air-Conditioning and Refrigeration 2012;20(1):1130002.

[6] Cheng Q, Xu WH. Performance analysis of a novel multi-function liquid desiccant regeneration system for liquid desiccant air-conditioning system. Energy 2017;140:240-252.

[7] Kabeel AE, Khalil A, Elsayed SS, Alatyar AM. Dynamic behaviour simulation of a liquid desiccant dehumidification system. Energy 2018;144:456-471.

[8] Liu XH, Chang XM, Xia JJ, Jiang Y. Performance analysis on the internally cooled dehumidifier using liquid desiccant. Building and Environment 2009;44(2):299-308.

[9] Rafique MM, Gandhidasan P, Bahaidarah HMS. Liquid desiccant materials and dehumidifiers-A review. Renewable Energy and Sustainable Review 2016;56:179-195.

[10] Chen XY, Jiang Y, Li Z, Qu KY. Field study on independent dehumidification air-conditioning system-I: performance of liquid desiccant dehumidification system. ASHRAE Transactions 2005;111(2):271-276.

[11] Dong CS, Qi RH, Lu L, Wang YL, Wang LS. Comparative performance study on liquid desiccant dehumidification with different packing types for built environment. Science and Technology for the Built Environment 2016;00:1-11.

[12] Chen Y, Yang HX, Luo YM. Investigation on solar assisted liquid desiccant dehumidifier and evaporative cooling system for fresh air treatment. Energy 2018;143:114-127.

[13] Xie Y, Zhang T, Liu XH. Performance investigation of a counter-flow heat pump driven liquid desiccant dehumidification system. Energy 2016;115:446-457.

[14] Bergero S, Chiari A. Performance analysis of a liquid desiccant and membrane contactor hybrid air-conditioning system. Energy and Buildings 2010;42(11):1976-1986.

[15] Cho YS, Kim SC, Kim YL, Kang YT. Combined heat and mass transfer analysis during the dehumidification process within a plate type heat exchanger. Journal of Mechanical Science and Technology 2013; 27:1875-1880.

[16] Yin YG, Zhang XS, Chen ZQ. Experimental study on dehumidifier and regenerator of liquid desiccant cooling air conditioning system. Building and Environment 2007;42(7):2505-2511.

[17] Luo YM, Wang M, Yang HX, Liu L, Peng JQ. Experimental study of the film thickness in the dehumidifier of a liquid desiccant air conditioning system. Energy 2015;84:239-246.

[18] Liu XH, Zhang Y, Qu KY, Jiang Y. Experimental study on mass transfer performances of cross flow dehumidifier using liquid desiccant. Energy Conversion and Management 2006;47:2682-2692.

[19] Liu J, Liu XH, Zhang T. Performance comparison of three typical types of internally-cooled liquid desiccant dehumidifiers. Building and Environment 2016;103:134-145.

[20] Yin YG, Zhang XS, Wang G, Luo L. Experimental study on a new internally cooled/heated dehumidifier/regenerator of liquid desiccant systems. International Journal of Refrigeration 2008;31:857-866.

[21] Dong CS, Lu L, Wen T. Experimental study on dehumidification performance enhancement by TiO_2 superhydrophilic coating for liquid desiccant plate dehumidifiers. Building and Environment 2017;124:219-231.

[22] Kessling W, Laevemann E, Kapfhammer C. Energy storage for desiccant cooling systems component development. Solar Energy 1998;64:209-221.

[23] Saman WY, Alizadeh S. An experimental study of a cross-flow type plate heat exchanger for dehumidification/cooling. Solar Energy 2002;73:59-71.

[24] Liu J, Zhang T, Liu XH, Jiang JJ. Experimental analysis of an internally-cooled/heated liquid desiccant dehumidifier/regenerator made of thermally conductive plastic. Energy and Buildings 2015;99:75-86.

[25] Owens DK, Wendt RC. Estimation of the surface free energy of polymers. Journal of Applied Polymer Science 1969;13(8):1741-1747.

[26] Żenkiewicz M. Methods for the calculation of surface free energy of solids. Journal of Achievements in Materials and Manufacturing Engineering 2007;24(1):137-145.

[27] Qi RH, Lu L, Yang HX, Qin F. Influence of plate surface temperature on the wetted area and system performance for falling film liquid desiccant regeneration system. International Journal of Heat and Mass Transfer 2013;64:1003-1013.

[28] Hui CM. Code of practice for overall thermal transfer value in buildings. Development Report. 2007.

[29] Qi RH, Lu L, Huang Y. Energy performance of solar-assisted liquid desiccant air-conditioning system for commercial building in main climate zones. Energy Conversion and Management 2014;88:749-757.